are generally hydrophobic and contain a small number of polar groups capable of hydrogen bonding. The unique composition of the ligand pocket not only allows hPXR to bind a diverse set of chemicals, but also (as seen with SR12813) permits a single ligand to dock in multiple orientations. This binding mode stands in sharp contrast to other nuclear receptor–ligand interactions, which have evolved to be highly specific. Because hPXR activation is responsible for an important class of drug-drug interactions, these structures may be useful for in silico screening of drug candidates to predict and avoid dangerous side effects.

References and Notes

1. S. A. Kliewer *et al.*, *Cell* **92**, 73 (1998).
2. J. M. Lehmann *et al.*, *J. Clin. Invest.* **102**, 1016 (1998).
3. G. Bertilsson *et al.*, *Proc. Natl. Acad. Sci. U.S.A.* **95**, 12208 (1998).
4. B. Blumberg *et al.*, *Genes Dev.* **12**, 3195 (1998).
5. W. Xie *et al.*, *Nature* **406**, 435 (2000).
6. P. Maurel, in *Cytochromes P450: Metabolic and Toxicological Aspects*, C. Ioannides, Ed. (CRC Press, Boca Raton, FL, 1996), pp. 241–270.
7. S. A. Jones *et al.*, *Mol. Endocrinol.* **14**, 27 (2000).
8. L. B. Moore *et al.*, *Proc. Natl. Acad. Sci. U.S.A.* **97**, 7500 (2000).
9. S. C. Piscitelli, A. H. Burstein, D. Chaitt, R. M. Alfaro, J. Falloon, *Lancet* **355**, 547 (2000).
10. F. Ruschitzka, P. J. Meier, M. Turina, T. F. Luscher, G. Noll, *Lancet* **355**, 548 (2000).
11. J. M. Wentworth, M. Agostini, J. Love, J. W. Schwabe, V. K. Chatterjee, *J. Endocrinol.* **166**, R11 (2000).
12. T. A. Berkhout *et al.*, *J. Biol. Chem.* **271**, 14376 (1996).
13. T. A. Berkhout *et al.*, *Atherosclerosis* **133**, 203 (1997).
14. J. Navaza, P. Saludjian, *Methods Enzymol.* **276A**, 581 (1997).
15. A. T. Brünger *et al.*, *Acta Crystallogr.* **D54**, 905 (1998).
16. D. Moras, H. Gronemeyer, *Curr. Opin. Cell Biol.* **10**, 384 (1998).
17. R. V. Weatherman, R. J. Fletterick, T. S. Scanlan, *Annu. Rev. Biochem.* **68**, 559 (1999).
18. N. Rochel, J. M. Wurtz, A. Mitschler, B. Klaholz, D. Moras, *Mol. Cell* **5**, 173 (2000).
19. W. Bourguet, M. Ruff, P. Chambon, H. Gronemeyer, D. Moras, *Nature* **375**, 377 (1995).
20. J.-P. Renaud *et al.*, *Nature* **378**, 681 (1995).
21. R. T. Nolte *et al.*, *Nature* **395**, 137 (1998).
22. S. P. Williams, P. B. Sigler, *Nature* **393**, 392 (1998).
23. A. K. Shiau *et al.*, *Cell* **95**, 927 (1998).
24. A. M. Brzozowski *et al.*, *Nature* **389**, 753 (1997).
25. For supplementary figures and tables, see *Science* Online (www.sciencemag.org/cgi/content/full/1060762/DC1).
26. R. T. Gampe Jr. *et al.*, *Mol. Cell* **5**, 545 (2000).
27. Placing single SR12813 molecules into the clear electron density in the PXR binding pocket resulted in adjacent positive electron density peaks, suggesting that more than one conformation of the ligand was present. This was confirmed using difference density generated from crystals of hPXR-LBD containing an iodinated form of SR12813 (I-SR12813), in which the two *t*-butyl groups of SR12813 were replaced with iodine. I-SR12813 was found to activate PXR as efficiently as did SR12813 (L. B. Moore, J. L. Collins, T. M. Willson, data not shown). Two difference density maps were used to guide positioning SR12813 ligands: $[(|F_{obs}^{I\text{-}SR12813}| - |F_{obs}^{SR12813}|), \phi_{calc}^{PROTEIN}]$ and $[(|F_{obs}^{I\text{-}SR12813}| - |F_{calc}^{PROTEIN}|), \phi_{calc}^{PROTEIN}]$, each calculated to 3.0 Å resolution (Table 1). Both maps showed a consistent set of significant positive difference density peaks (the highest peaks in both maps) in the ligand-binding pocket, which were interpreted to be the iodine atoms. Three SR12813 ligands optimally satisfied the electron density in the binding pocket: Position 1 was placed on the basis of two 7σ difference density peaks observed in both maps, position 3 on the basis of two 5σ difference density peaks, and position 2 on the basis of two 4σ difference density peaks. Occupancies of each ligand position were estimated on the basis of iodine difference density and standard electron density peaks, and were fixed at 0.4, 0.2, and 0.4 for positions 1, 2, and 3, respectively.
28. B. Goodwin, E. Hodgson, C. Liddle, *Mol. Pharmacol.* **56**, 1329 (1999).
29. U. Savas, M. R. Wester, K. J. Griffin, E. F. Johnson, *Drug Metab. Disp.* **28**, 529 (2000).
30. Residues 130 to 434 of hPXR-LBD were engineered as an NH_2-terminal polyhistidine-tagged fusion protein and subcloned into the pRSETA expression vector (Invitrogen). Residues 623 to 710 of the human SRC-1 protein were subcloned into the bacterial vector pACYC184 (American Type Culture Collection 37033) along with a T7 promoter (*21*). The hPXR-LBD–pRSETA and SRC-1–pACYC184 plasmids were cotransformed into the BL21(DE3) strain of *Escherichia coli* and expressed with isopropyl-β-D-thiogalactopyranoside in shaker flasks at 22°C. Cell pellets were resuspended, lysed by sonication, and clarified by centrifugation. The cleared supematant was loaded onto ProBond nickel-chelating resin (Invitrogen). The PXR-LBD–SRC-1 complex was eluted using 500 mM imidazole (pH 7.5). Fractions were pooled, concentrated using Centri-prep 30K (Amicon) units, and subjected to size exclusion using Sepharose S-75 resin (Pharmacia). Column fractions containing the PXR–SRC-1 complex were pooled and loaded onto a 50-ml Mono-S Sepharose Fast Flow column (Pharmacia). The protein complex was eluted from the column at 300 mM NaCl in an increasing salt gradient. The appropriate column fractions, which contained the 1:1 PXR–SRC-1 complex, were pooled and stored on ice. Purity for the PXR–SRC-1 complex was estimated at >95%, as assessed by SDS–polyacrylamide gel electrophoresis (PAGE) with silver staining.
31. S. A. Onate, S. Y. Tsai, M. J. Tsai, B. W. O'Malley, *Science* **270**, 1354 (1995).
32. A. T. Brünger, *Acta Crystallogr.* **D49**, 24 (1993).
33. T. A. Jones, J. Y. Zou, S. W. Cowan, M. Kjeldgaard, *Acta Crystallogr.* **A47**, 110 (1991).
34. R. J. Read, *Acta Crystallogr.* **A42**, 140 (1986).
35. P. J. Kraulis, *J. Appl. Crystallogr.* **24**, 946 (1991).
36. E. A. Merritt, D. J. Bacon, *Methods Enzymol.* **277**, 505 (1997).
37. A. Nicholls, K. A. Sharp, B. Honig, *Proteins* **11**, 281 (1991).
38. L. B. Moore *et al.*, *J. Biol. Chem.* **275**, 15122 (2000).

39. We thank B. Bernstein and R. Thapar for critical comments on the manuscript; P. Kuhn, M. Soltis (Stanford Synchrotron Radiation Facility), A. Howard, L. Keefe (Advanced Photon Source), E. Collins, and L. Betts for assistance with data collection; J. Shenk for experimental assistance; and members of the Redinbo group, including Y. Xue, J. Chrencik, T. Thieu, S. Bencharit, and E. Howard-Williams, for experimental and data collection assistance. Supported by a Glaxo-UNC Collaborative Research Grant, the UNC Lineberger Comprehensive Cancer Center, and a Burroughs Wellcome Career Award in the Biomedical Sciences (M.R.R.). Coordinates for the apo and SR12813-bound forms of hPXR-LBD have been deposited with the Research Collaboratory for Structural Bioinformatics and assigned Protein Data Bank accession codes 1ILG and 1ILH, respectively.

16 March 2001; accepted 11 May 2001
Published online 14 June 2001;
10.1126/science.1060762
Include this information when citing this paper.

Recruitment of HAT Complexes by Direct Activator Interactions with the ATM-Related Tra1 Subunit

Christine E. Brown,[1,2] LeAnn Howe,[1,2] Kyle Sousa,[1,2] Stephen C. Alley,[3] Michael J. Carrozza,[1,2] Song Tan,[2] Jerry L. Workman[1]*

Promoter-specific recruitment of histone acetyltransferase activity is often critical for transcriptional activation. We present a detailed study of the interaction between the histone acetyltransferase complexes SAGA and NuA4, and transcription activators. We demonstrate by affinity chromatography and photo–cross-linking label transfer that acidic activators directly interact with Tra1p, a shared subunit of SAGA and NuA4. Mutations within the COOH-terminus of Tra1p disrupted its interaction with activators and resulted in gene-specific transcriptional defects that correlated with lowered promoter-specific histone acetylation. These data demonstrate that the essential Tra1 protein serves as a common target for activators in both SAGA and NuA4 acetyltransferases.

The recruitment of histone acetyltransferase complexes to genomic loci via direct interactions with transcriptional activators is important for the regulation of gene expression (*1*). We have previously shown that two yeast histone acetyltransferase (HAT) complexes, SAGA and NuA4, specifically interact with acidic activation domains and selectively stimulate transcription driven by these activators from chromatin templates in vitro (*2–4*). The 1.8-megadalton (MD) SAGA complex contains at least 14 subunits, and preferentially

[1]Howard Hughes Medical Institute, [2]Department of Biochemistry and Molecular Biology, [3]Department of Chemistry, The Pennsylvania State University, 306 Althouse Laboratory, University Park, PA 16802, USA.

*To whom correspondence should be addressed: E-mail: jlw10@psu.edu

acetylates histone H3 (*5*). The 1.3-MD NuA4 complex contains at least 11 subunits and preferentially acetylates histone H4 (*5*). To understand the mechanism by which activators specifically recruit SAGA and NuA4, the identification of the activator target(s) within these HAT complexes is critical.

SAGA and NuA4 exhibit a similar preference for interacting with acidic activation domains of the herpes virus VP16 and yeast Gcn4 proteins [Fig. 1A and (*2*, *6*)]. The propensity of these complexes to interact with a similar set of acidic activators is further supported by the coprecipitation of SAGA (Fig. 1A, upper panel) and NuA4 (Fig. 1A, middle panel) HAT activity with glutathione *S*-transferase (GST) fusions of the yeast Gal4 and Hap4 acidic activation domains. The region of each activation domain utilized in these studies has been shown to be sufficient for transcriptional activation both in vitro and in vivo (*7*–*9*). Mutant activation domains VP16Δ456 and gcn4(5,7) are dramatically compromised in their ability to coprecipitate SAGA and NuA4 HAT activity (Fig. 1A, lanes 7 and 11), a finding that correlates with the reduced transcriptional potency of these domains (*7*, *10*). Our results demonstrate that SAGA and NuA4 can interact with a similar set of acidic transcriptional activators and exhibit comparable specificity, suggesting that the underlying mechanism for activator interaction may be similar.

To identify subunits within the native SAGA and NuA4 complexes mediating their interaction with activators, we used a photo–cross-linking label transfer strategy (*11*). The advantage of this approach is that the activator target(s) can be identified within the context of the intact HAT complex. We utilized two related photo–cross-linking agents, which differ only in the reactive group for conjugation to a bait protein (lysine-reactive Sulfo-SBED and cysteine-reactive SCA2) (Fig. 1B). GST-HAP4 was chosen as the bait protein, because it is the only activator in our study that contains a cysteine (1 C) and multiple lysines (14 K). In the presence of ultraviolet (UV) irradiation, the biotin moiety was transferred from both the K and C derivatized HAP4 to a large protein of ~400 kD in both the SAGA- and NuA4-containing reactions (Fig. 1C). The only known subunit to be shared between SAGA and NuA4 is the 434-kD Tra1 protein (*12*, *13*), and Tra1p can be unambiguously identified as a target, because it is well separated from all other SAGA and NuA4 subunits (>200 kD larger). A second label transfer to an ~80-kD polypeptide in the SAGA-containing reactions is sometimes observed, and the identity of this protein is currently being pursued. The background observed in this assay is independent of the addition of HAT complex and presumed to be due to the dimerization of GST-HAP4. This background precluded the detection of other possible activator targets, particularly between 50 and 66 kD (see below). However, the label transfer occurring between HAP4 and Tra1p implicates Tra1p as a direct target of activators in SAGA and NuA4.

The essential Tra1 protein (*14*) is homologous to human TRRAP (*15*), a protein component of the SAGA-related HAT complexes PCAF, TFTC, and STAGA and the NuA4-related TIP60 HAT complex (*5*). TRRAP was originally identified biochemically as a cofactor that was purified from HeLa nuclear extracts via a c-Myc affinity column, and found to be necessary for c-Myc–dependent cell transformation (*15*). To confirm a direct interaction between Tra1p and activators, purified Tra1p (*11*, *16*) was used in GST pull-down assays with the activators presented above (Fig. 2A). The purified Tra1 protein efficiently coprecipitated with wild-type activation domains of VP16, GCN4, GAL4, and HAP4, but not with the VP16Δ456 and gcn4(5,7) mutants (Fig. 2B). These results show that Tra1p interacts with activation domains with the same specificity as native SAGA and NuA4 (see Fig. 1A). Together, the cross-linking and pull-down studies establish that Tra1p is an important mediator of HAT-activator interaction.

The *Drosophila* and human homologs of the yeast SAGA subunit $TAF_{II}17$ ($dTAF_{II}40$ and $hTAF_{II}31$, respectively) have been shown to interact with acidic activators when expressed individually (*17*–*20*). Thus, the smaller yeast $TAF_{II}17$ protein represented a potential activator target in SAGA. To examine this possibility, a SAGA TAF_{II}-Ada1p subcomplex (consisting of $TAF_{II}17$, $TAF_{II}60$, and histone-fold domains of $TAF_{II}61$ and Ada1p) were coexpressed in *Escherichia coli*, purified to homogeneity (Fig. 2C) (*21*, *22*), and tested for activator interactions. As shown in Fig. 2D (upper panel), specific interactions between the TAF_{II}-Ada1p complex and acidic activation domains were not detected. Consistent

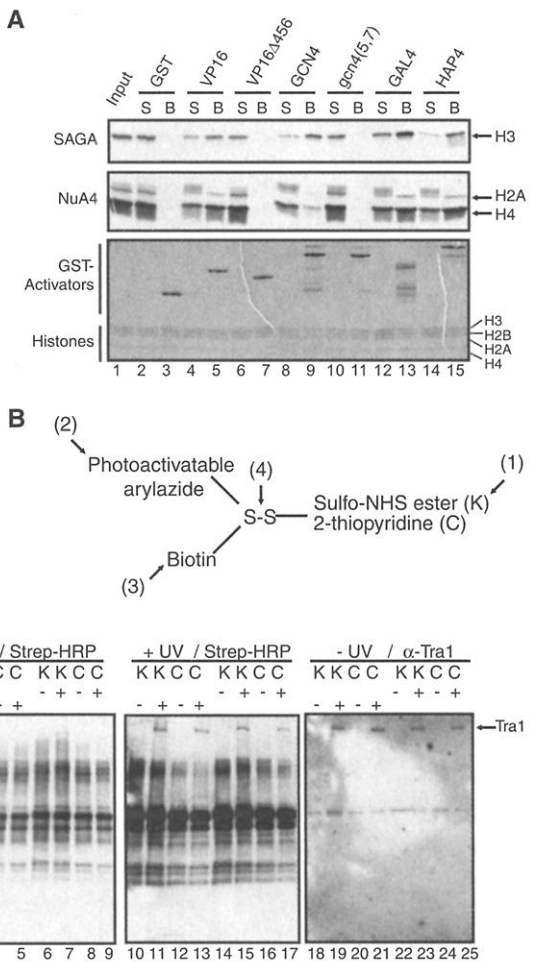

Fig. 1. (**A**) Coprecipitation assays performed with Superose 6–purified SAGA and NuA4 HAT complexes and 3 μg of GST or GST activator fusions VP16, VP16Δ456, GCN4, gcn4(5,7), GAL4, and HAP4 (*11*). Equal amounts of input, supernatant (S), and glutathione-Sepharose bound (B) fractions were assayed for HAT activity (*30*). Top panel, fluorograms of SAGA-dependent core histone HAT activity. Middle panel, fluorograms of NuA4-dependent nucleosomal HAT activity. Bottom panel, Coomassie blue staining of upper panel gel showing levels of precipitated GST-activator fusions and core histone substrates. (**B**) Schematic of tetrafunctional cross-linking reagents Sulfo-SBED (Pierce) and SCA2 (*35*) with cross-linking distances of 21 Å and 17 Å, respectively. Numbers on scheme are as follows: (1), reactive group for conjugation to bait protein at lysine (K) residues (Sulfo-SBED) or cysteine (C) residues (SCA2); (2), photactivatable arylazide; (3), biotin moiety detectable by streptavidin–horseradish peroxidase (HRP); (4), disulfide linkage reducible by dithiothreitol (DTT). (**C**) Photo–cross-linking analysis of GST-HAP4 (~0.6 pmol), conjugated with Sulfo-SBED (K) or SCA2 (C) and purified SAGA and NuA4 (~0.3 pmol) (*11*). Reactions were separated by 4 to 15% SDS–polyacrylamide gel electrophoresis (SDS-PAGE) and blotted to polyvinylidene difluoride (PVDF) membrane. Left panel, streptavidin-HRP probed blot of reactions incubated in the absence of UV irradiation. Biotinylated protein markers (New England Biolabs) are shown in lane 1. Middle panel, streptavidin-HRP–probed blot of reactions irradiated with UV light for 10 min at room temperature and reduced with 100 mM DTT. Right panel, left blot (−UV) was reprobed with Tra1p antibody.

with this finding, we did not detect a label transfer to $TAF_{II}17$ in the cross-linking studies (Fig. 1C). Thus, although it remains possible that $TAF_{II}17$ participates in activator interactions in vivo (perhaps as a modified protein or within TFIID), when incorporated into a SAGA subcomplex, it fails to bind activators under conditions where Tra1p binds efficiently.

The Ada2p subunit of SAGA has also been shown to interact with acidic activators when expressed individually (*23*, *24*). We tested the ability of Ada2p, within the context of its interaction partners Ada3p and Gcn5p (*25*, *26*), to associate with activators. The recombinant Ada2p-Ada3p-Gcn5p trimeric complex (Fig. 2C, lane 4) can efficiently acetylate nucleosomal and core histone substrates, and it exhibits acetylase activity comparable to the intact SAGA complex (*27*). However, in contrast to the results with Tra1p, the recombinant Ada2p-Ada3p-Gcn5p trimeric complex failed to demonstrate specific interactions with acidic activators (Fig. 2D, lower panel). In addition, we have found that mutant SAGA complexes lacking Ada2p retain the ability to interact with activators (*11*). These results are consistent with the observation that the ADA HAT complex containing Ada2p, Ada3p, and Gcn5p, but not Tra1p, is unable to interact with acidic activators (*2*). Furthermore, we find that Gcn5p-dependent histone acetylation is required for the toxic effects of GAL4-VP16 overexpression in yeast (*11*). We suggest that *ADA2*, *ADA3*, and *GCN5* were identified in the VP16 toxicity screen because they are required for the nucleosomal HAT activity of SAGA (*27*), not because of their contacts with activators (*11*). These results strongly suggest that Tra1p plays a more important role in activator interactions of the SAGA complex than does Ada2p.

To gain further insight into *TRA1* function, we isolated six temperature-sensitive alleles. The majority of the *tra1* temperature-sensitive alleles resulted in a dramatic reduction of Tra1 protein levels at the restrictive

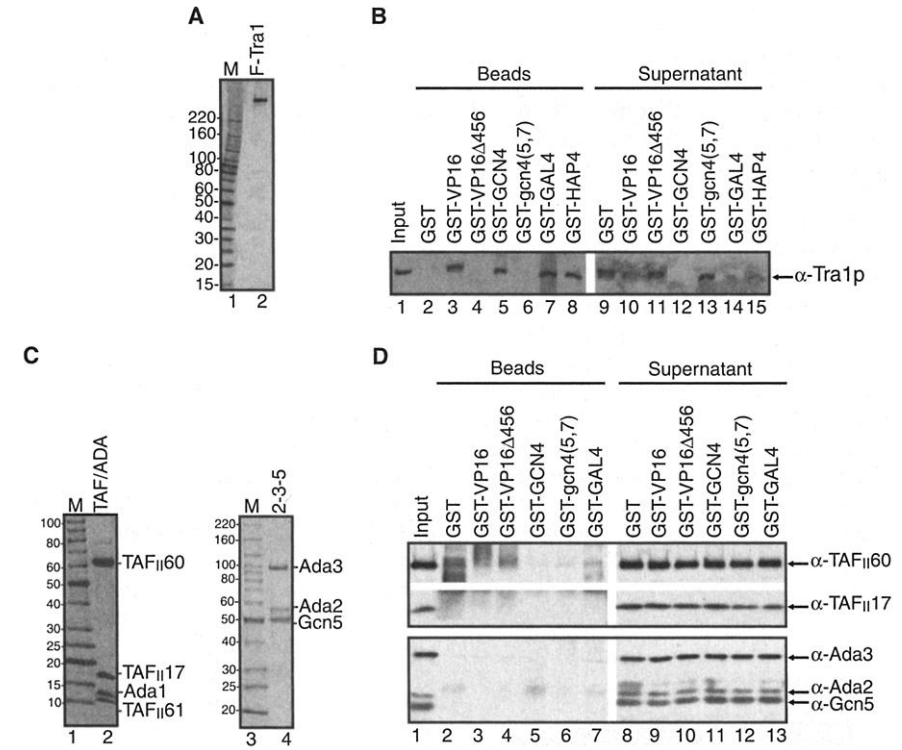

Fig. 2. (**A**) Silver-stained SDS-PAGE gel of Flag-Tra1p purified from yeast extracts (*11*) (lane 2). BenchMark protein molecular mass standards (Gibco-BRL) (lane 1). (**B**) GST-activator (~10 μg fusion protein) coprecipitation assays with purified Flag-Tra1p (*11*). Equal amounts of input, supernatant, and bead fractions were immunoprobed with the antibody against Tra1p (α-Tra1). (**C**) Coomassie blue–stained SDS-PAGE gel of recombinant SAGA histone-fold subcomplex [full-length $TAF_{II}60$ and $TAF_{II}17$; histone-fold domains of $TAF_{II}61$ and Ada1p (*21*, *22*)] (lane 2). Coomassie blue staining of recombinant SAGA trimeric complex [full-length Ada2p, Ada3p, and Gcn5p (*27*)] (lane 4). Lanes 1 and 3, BenchMark protein molecular mass standards (Gibco-BRL). (**D**) GST-activator coprecipitation assays (~10 μg recombinant protein cross-linked to glutathione-Sepharose) were performed with the TAF_{II}-Ada1p histone-fold complex (upper panel), and the Ada3-Ada2-Gcn5p trimeric complex (lower panel) (*11*). Equal amounts of input, supernatant, and bead fractions were immunoprobed with the indicated antibody.

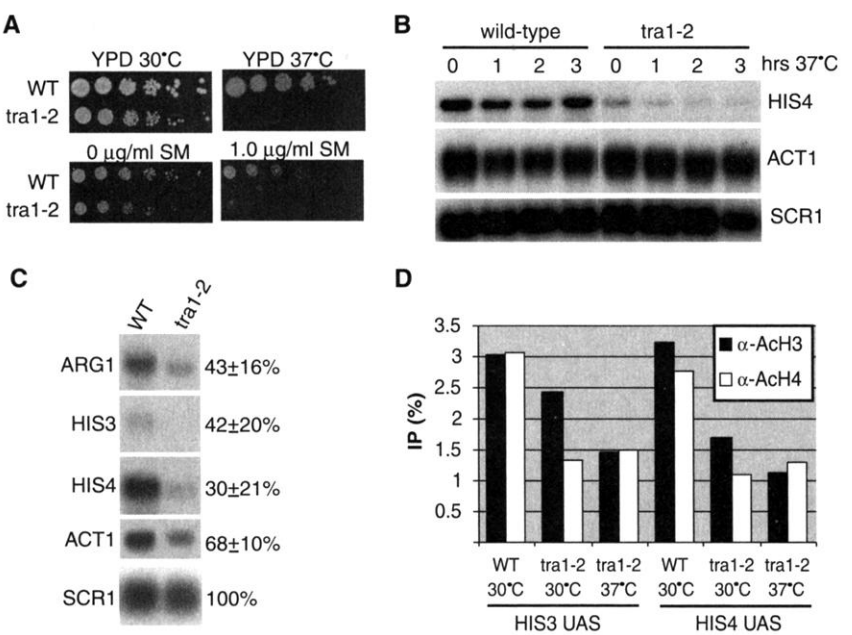

Fig. 3. (**A**) Dilutions (fourfold starting at an optical density at 600 nm of 0.16) of wild-type (WT) and *tra1-2* strains were spotted onto plates with yeast extract, peptone, and dextrose (YPD), then grown at 30°C and 37°C for 2 days, or yeast nitrogen base and dextrose (YMD) plates with and without 1 μg/ml sulfometuron methyl (SM) (grown at 30°C for 3 days). (**B**) Northern analysis of wild-type and *tra1-2* strains grown in minimal medium at 30°C and shifted to 37°C for 3 hours. (**C**) Northern analysis of wild-type and *tra1-2* strains grown in minimal medium at 30°C. RNA loading was standardized to scR1, and the percentage decrease in the *tra1-2* mutant as compared with wild-type is reported to the right (average of three experiments). (**D**) Quantification of chromatin immunoprecipitation experiments performed with anti-acetylated H3 and H4 antibodies (Upstate Biotechnology) (*11*) with extracts prepared from wild-type and *tra1-2* strains grown at 30°C or shifted to 37°C for 3 hours. Slot blots were probed with fragments corresponding to the *HIS3 UAS* and *HIS4 UAS* (*11*), and quantification of chromatin IP experiment is reported as a percentage of immunoprecipitated material.

temperature (37°C) (*28*). In contrast, the protein levels of one temperature-sensitive allele, termed *tra1-2*, remained unchanged even at the restrictive temperature [0 to 4 hours at 37°C (*28*)]. SAGA and NuA4 complex integrity and HAT activity appear to be intact at both the permissive and nonpermissive temperature in the *tra1-2* mutant (*28*). However, yeast-expressing tra1-2p exhibited phenotypes consistent with compromised Gcn4p-dependent transcription. First, growth of the *tra1-2* strain is sensitive to sulfometuron methyl (Fig. 3A), an inhibitor of isoleucine and valine biosynthesis, and a derepressor of the Gcn4p-regulated genes (*29*). Second, a time course at 37°C revealed that *HIS4* transcript levels are reduced in the *tra1-2* mutant (Fig. 3B). Third, the *tra1-2* mutant grown at the permissive temperature exhibits an ~50% reduction in steady-state RNA levels of Gcn4p-regulated genes *ARG1*, *HIS3*, and *HIS4* as compared with *ACT1* and *SCR1* (RNA pol III gene) (Fig. 3C). Finally, in vivo chromatin immunoprecipitation studies revealed a lower level of histone H3 and H4 acetylation at the *HIS3* and *HIS4* upstream activating sequence (UAS) regions in the *tra1-2* mutant. Reduced levels of acetylation were detected at the permissive temperature, and after 3 hours at the nonpermissive temperature, both H3 and H4 acetylation levels were decreased by about half to one-third [Fig. 3D and (*11*)].

Given the observed defects for the *tra1-2* mutant in Gcn4p-dependent transcription and promoter acetylation, we explored the possibility that mutations within tra1-2p decrease the efficiency with which activators can recruit SAGA and NuA4 to promoters. Consistent with this hypothesis, we found that the tra1-2 protein was defective in its ability to interact with activators. For these experiments, HAT complexes were enriched by Ni-agarose chromatography (*30*) and tested for the ability to interact with GST-VP16. Reduced interaction was observed for the tra1-2 protein at the permissive temperature, and further reduction occurred with extracts prepared at the restrictive temperature (Fig. 4B). Sequencing of the *tra1-2* allele identified seven point mutations, five of which reside within the COOH-terminal half of the protein (Fig. 4A). This suggested that the activator interaction domain (AID) might be contained within the COOH-terminus. To test this possibility, the COOH-terminal regions (amino acids 2226 to 3744) of wild-type Tra1p and tra1-2p were produced by in vitro translation and tested for the ability to interact with VP16 (*11*). As shown in Fig. 4C, only the wild-type COOH-terminal fragment was capable of interacting with VP16, but not the fragment derived from the mutant tra1-2 protein. Moreover, a deletion within this domain (Δ2233 to 2836 amino acids) in the context of the full-length Tra1 protein (*11*) dramatically reduced the ability of Tra1p to interact with VP16 (Fig. 4D). These results suggest that the COOH-terminal region of Tra1p directly mediates the observed interaction with activators.

In summary, we have identified Tra1p as a direct target of activators within the NuA4 and SAGA HAT complexes. We have shown that mutations within *TRA1* resulted in decreased interaction with acidic activators, gene-specific transcriptional defects, and decreased acetylation levels at Gcn4p-regulated genes. Our findings suggest that Tra1p defines a general mechanism by which SAGA and NuA4 interact with acidic activators. These results suggest that SAGA and NuA4 might be recruited by a similar set of yeast activators to a common set of promoters. In support of this hypothesis, mutations in SAGA and NuA4 decrease the expression of a subset of Gcn4p- and Pho4p-regulated genes (*31–33*). However, it is important to note that SAGA and NuA4 are unlikely to have identical roles in transcription. Even if an activator recruits both SAGA and NuA4, these HATs acetylate discrete histones substrates (H3-H2B and H4-H2A, respectively), and thus likely have some distinct functions with respect to transcriptional activation. It remains possible that other subunits within SAGA and NuA4 increase the HAT-activator interaction or alter activator specificity in a Tra1p-independent manner.

TRRAP-dependent hGcn5 recruitment has been shown to be essential for the c-Myc oncogenic activity (*34*). In light of this and our results, we envisage that the Tra1p-dependent recruitment of acetyltransferase activity is critical for the regulation of gene expression.

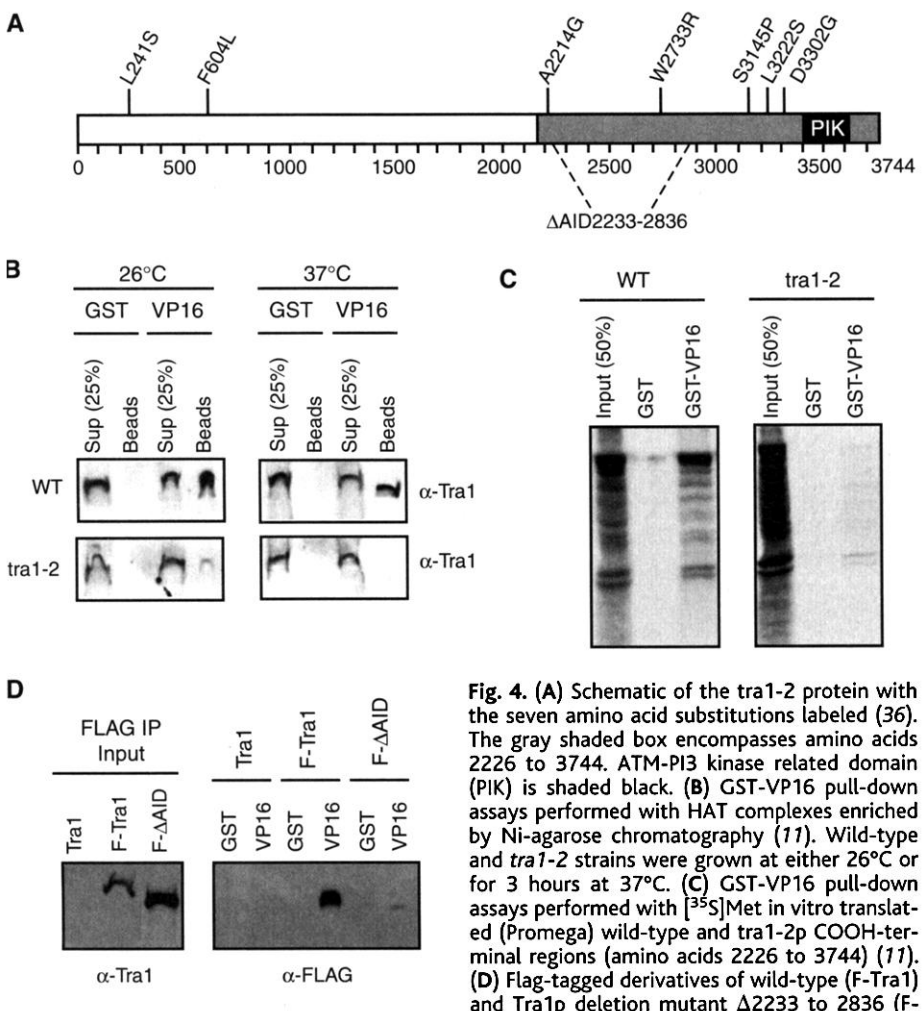

Fig. 4. (**A**) Schematic of the tra1-2 protein with the seven amino acid substitutions labeled (*36*). The gray shaded box encompasses amino acids 2226 to 3744. ATM-PI3 kinase related domain (PIK) is shaded black. (**B**) GST-VP16 pull-down assays performed with HAT complexes enriched by Ni-agarose chromatography (*11*). Wild-type and *tra1-2* strains were grown at either 26°C or for 3 hours at 37°C. (**C**) GST-VP16 pull-down assays performed with [^{35}S]Met in vitro translated (Promega) wild-type and tra1-2p COOH-terminal regions (amino acids 2226 to 3744) (*11*). (**D**) Flag-tagged derivatives of wild-type (F-Tra1) and Tra1p deletion mutant Δ2233 to 2836 (F-ΔAID) were expressed in the wild-type yeast strain (YJW100) on a high-copy vector. FLAG(M2)-Sepharose and GST-VP16 coprecipitation assays were performed with 200 μg of yeast whole-cell extract (*11*).

References and Notes

1. J. L. Workman, R. E. Kingston, *Annu. Rev. Biochem.* **67**, 545 (1998).
2. R. T. Utley *et al.*, *Nature* **394**, 498 (1998).
3. M. Vignali, D. J. Steger, K. E. Neely, J. L. Workman, *EMBO J.* **19**, 2629 (2000).
4. K. Ikeda, D. J. Steger, A. Eberharter, J. L. Workman, *Mol. Cell. Biol.* **19**, 855 (1999).
5. C. E. Brown, T. Lechner, L. Howe, J. L. Workman, *Trends Biochem. Sci.* **25**, 15 (2000).

6. Slightly diminished NuA4 HAT activity is detected on the GST-GCN4 beads relative to SAGA. However, this difference does not appear to be due to a decreased interaction between NuA4 and Gcn4p (*2*, *28*), but instead to a decrease in nucleosomal HAT activity when bound to GST-GCN4.
7. C. M. Drysdale *et al.*, *Mol. Cell. Biol.* **15**, 1220 (1995).
8. S. L. Berger *et al.*, *Cell* **70**, 251 (1992).
9. A. K. Sil *et al.*, *Mol. Cell. Biol.* **19**, 7828 (1999).
10. S. L. Berger, W. D. Cress, A. Cress, S. J. Triezenberg, L. Guarente, *Cell* **61**, 1199 (1990).
11. Complete experimental protocols and other information are available as supplementary material on *Science* Online at www.sciencemag.org/cgi/content/full/292/5525/2333/DC1.
12. S. Allard *et al.*, *EMBO J.* **18**, 5108 (1999).
13. P. A. Grant, D. Schieltz, M. G. Pray-Grant, J. R. R. Yates, J. L. Workman, *Mol. Cell* **2**, 863 (1998).
14. A. Saleh *et al.*, *J. Biol. Chem.* **273**, 26559 (1998).
15. S. B. McMahon, H. A. Van Buskirk, K. A. Dugan, T. D. Copeland, M. D. Cole, *Cell* **94**, 363 (1998).
16. Several lines of evidence support the assumption that purified Flag-Tra1p is free of SAGA and NuA4 subunits (*28*). First, elution of Flag-Tra1p from MonoQ is chromatographically distinct from NuA4 and SAGA. Second, the purified protein does not contain any histone acetylase activity. Third, the purified Flag-Tra1p fraction does not contain the SAGA subunits Spt7p, $TAF_{II}90$, Spt8p, and Ada2p and the NuA4 catalytic subunit Esa1p, as determined by Western blot analysis. Two smaller proteins at 85 and 35 kD are sometimes observed in this fraction. Mass spectrometry and Western analysis suggest that these are Tra1p breakdown products.
17. H. Lu, A. J. Levine, *Proc. Natl. Acad. Sci. U.S.A.* **92**, 5154 (1995).
18. M. Uesugi, O. Nyanguile, H. Lu, A. J. Levine, G. L. Verdine, *Science* **277**, 1310 (1997).
19. C. J. Thut, J. L. Chen, R. Klemm, R. Tjian, *Science* **267**, 100 (1995).
20. J. A. Goodrich, T. Hoey, C. J. Thut, A. Admon, R. Tjian, *Cell* **75**, 519 (1993).
21. W. Selleck *et al.*, *Nature Struct. Biol.*, in press.
22. W. Selleck, S. Tan, unpublished data.
23. N. A. Barlev *et al.*, *J. Biol. Chem.* **270**, 19337 (1995).
24. A. Henriksson *et al.*, *Mol. Cell. Biol.* **17**, 3065 (1997).
25. R. Candau, J. X. Zhou, C. D. Allis, S. L. Berger, *EMBO J.* **16**, 555 (1997).
26. R. Candau, S. L. Berger, *J. Biol. Chem.* **271**, 5237 (1996).
27. R. Balasubramanian, W. Selleck, M. G. Pray-Grant, P. Grant, S. Tan, in preparation.
28. C. Brown, J. Workman, unpublished data.
29. M. H. Jia *et al.*, *Physiol. Genomics* **3**, 83 (2000).
30. A. Eberharter, S. John, P. A. Grant, R. T. Utley, J. L. Workman, *Methods* **15**, 315 (1998).
31. P. D. Gregory, A. Schmid, M. Zavari, M. Munsterkotter, W. Horz, *EMBO J.* **18**, 6407 (1999).
32. L. Galarneau *et al.*, *Mol. Cell* **5**, 927 (2000).
33. M.-H. Kuo, J. Zhou, P. Jambeck, M. E. A. Churchill, C. D. Allis, *Genes Dev.* **12**, 627 (1998).
34. S. B. McMahon, M. A. Wood, M. D. Cole, *Mol. Cell. Biol.* **20**, 556 (2000).
35. S. C. Alley, F. T. Ishmael, A. D. Jones, S. J. Benkovic, *J. Am. Chem. Soc.* **122**, 6126 (2000).
36. Single-letter abbreviations for the amino acid residues are as follows: A, Ala; D, Asp; F, Phe; G, Gly; L, Leu; R, Arg; S, Ser; T, Thr; V, Val; and W, Trp.
37. We thank K. Neely, M. Swanson, A. Hinnebusch, F. Ishmael, R. Balasubramanian, and W. Selleck for helpful discussions and sharing of reagents. C.E.B. is supported by the Leukemia and Lymphoma Society. S.C.A. is supported by NIH grant GM19492. J.L.W. is an Associate Investigator of the Howard Hughes Medical Institute. This work was supported by a grant from NIGMS.

11 December 2000; accepted 15 May 2001

Requirement of ERK Activation for Visual Cortical Plasticity

Graziella Di Cristo,[1]* Nicoletta Berardi,[2,3]† Laura Cancedda,[1] Tommaso Pizzorusso,[1,2] Elena Putignano,[1] Gian Michele Ratto,[2] Lamberto Maffei[1,2]

Experience-dependent plasticity in the developing visual cortex depends on electrical activity and molecular signals involved in stabilization or removal of inputs. Extracellular signal–regulated kinase 1,2 (also called p42/44 mitogen-activated protein kinase) activation in the cortex is regulated by both factors. We show that two different inhibitors of the ERK pathway suppress the induction of two forms of long-term potentiation (LTP) in rat cortical slices and that their intracortical administration to monocularly deprived rats prevents the shift in ocular dominance towards the nondeprived eye. These results demonstrate that the ERK pathway is necessary for experience-dependent plasticity and for LTP of synaptic transmission in the developing visual cortex.

During development, experience exerts a strong control over formation of circuitry in sensory cortices, promoting the strengthening or weakening of synapses. For example, monocular deprivation (MD) during the critical period determines a loss of responsiveness to the deprived eye in visual cortical neurons. Molecules controlling experience-dependent plasticity during the critical period (*1*–*3*) should be regulated by electrical activity (*4*, *5*) and by other factors, such as neurotrophins (*6*–*8*), important for cortical plasticity. Electrical activity and neurotrophins are among the strongest activators of ERK (*9*, *10*), suggesting that ERK could act as an integrating molecule between these two regulatory mechanisms. ERK is also implicated in activity-dependent plasticity by studies of learning and memory (*11*–*14*). We investigated the role of ERK in experience-dependent plasticity of the visual cortex and on LTP, an in vitro model of activity-dependent synaptic plasticity [see Web material (*15*) for methods].

The effect of specific inhibitors (*16*) of the ERK pathway (U0126 and PD98059) on LTP induction was studied in visual cortical slices. A stimulating electrode was placed in layer IV, and field potentials (FPs) were evoked by a brief current pulse (100 μs) delivered every 30 s and recorded in layer III (*17*). Stimulus intensity was 55 ± 9% of that evoking the maximal response. In normal saline, theta burst stimulation (TBS) delivered to layer IV induced a potentiation of the response [FP amplitude 25 min after TBS (as percentage of pre-TBS baseline), 120.0 ± 2.8%; $n = 7$].

To assess the effects of ERK pathway inhibitors on LTP, slices obtained from the same animal (P26 to P33) were treated 10 min before TBS with the blocker or its vehicle [dimethyl sulfoxide (DMSO) 0.1%]. Administration of U0126 (20 μM, a specific inhibitor of the upstream enzymes MEK that activate ERK) prevented LTP induction (Fig. 1): FP amplitude in U0126 treated slices remained at pre-TBS levels (99.4 ± 4.3%). In contrast, control slices displayed normal LTP (119.1 ± 3.7%). Change in FP amplitude 25 min after TBS is reported in Fig. 1C for each slice (U0126 treated or control). The time course of the response amplitude of U0126 treated slices differs from controls immediately after TBS delivery (Fig. 1A). The rapidity of the onset of U0126 effect suggests that ERK action is required for mechanisms of potentiation that, at least initially, are independent of gene transcription. The inhibitory effect of U0126 on LTP was not caused by reduced responses to the TBS or by antagonization of *N*-methyl-D-aspartate (NMDA)–mediated synaptic transmission, a key event for the induction of this form of LTP (*15*).

To exclude that LTP suppression by U0126 was due to a nonspecific interaction with molecules other than MEK, we tested a different MEK inhibitor, PD98059; 10-min incubation in 50 μM PD98059 totally suppressed LTP induction (Fig. 1C). Thus, inhibition of ERK signalling prevented LTP induction in the layer IV–III pathway.

FPs recorded in layer III after stimulation of white matter (WM) can also be potentiated by TBS. However, unlike layer IV-III LTP, which can be elicited through the entire lifetime, WM LTP is present only during the critical period. This observation suggested that this form of synaptic plasticity might be

[1]Scuola Normale Superiore, Piazza Cavalieri, 7 56126 Pisa, Italy. [2]Istituto Neurofisiologia CNR, via Moruzzi 1, 56100 Pisa, Italy. [3]Dipartimento di Psicologia, Università di Firenze, 50123 Firenze, Italy.

*Present address: Department of Neurobiology, Cold Spring Harbor Laboratory, Post Office Box 100, 1 Bungtown Road, Cold Spring Harbor, NY 11724, USA. †To whom correspondence should be addressed. E-mail: berardi@in.pi.cnr.it